Published in final edited form as:
Biochem Pharmacol. 2009 November 1; 78(9): 1105–1114. doi:10.1016/j.bcp.2009.06.009.

N-Myc down regulation induced differentiation, early cell cycle exit, and apoptosis in human malignant neuroblastoma cells having wild type or mutant p53

Rajiv Janardhanan[1], **Naren L. Banik**[2], and **Swapan K. Ray**[1,*]

[1] Department of Pathology, Microbiology, and Immunology, University of South Carolina School of Medicine, 6439 Garners Ferry Road, Columbia, SC 29209, USA

[2] Department of Neurosciences, Medical University of South Carolina, 96 Jonathan Lucas Street, P.O. Box 250606, Charleston, SC 29425, USA

Abstract

Neuroblastomas, which mostly occur in children, are aggressive metastatic tumors of the sympathetic nervous system. The failure of the previous therapeutic regimens to target multiple components of N-Myc pathway resulted in poor prognosis. The present study investigated the efficacy of the combination of N-(4-hydroxyphenyl) retinamide (4-HPR, 0.5 μM) and genistein (GST, 25 μM) to control the growth of human neuroblastoma cells (SH-SY5Y and SK-N-BE2) harboring divergent molecular attributes. Combination of 4-HPR and GST down regulated N-Myc, Notch-1, and Id2 to induce neuronal differentiation. Transition to neuronal phenotype was accompanied by increase in expression of e-cadherin. Induction of neuronal differentiation was associated with decreased expression of hTERT, PCNA, survivin, and fibronectin. This is the first report that combination of 4-HPR and GST mediated reactivation of multiple tumor suppressors (p53, p21, Rb, and PTEN) for early cell cycle exit (due to G1/S phase arrest) in neuroblastoma cells. Reactivation of tumor suppressor(s) repressed N-Myc driven growth factor mediated angiogenic and invasive pathways (VEGF, b-FGF, MMP-2, and MMP-9) in neuroblastoma. Repression of angiogenic factors led to the blockade of components of mitogenic pathways [phospho-Akt (Thr 308), p65 NF-κB and p42/44 Erk 1/2]. Taken together, the combination of 4-HPR and GST effectively blocked survival, mitogenic, and angiogenic pathways and activated proteases for apoptosis in neuroblastoma cells. These results suggested that combination of 4-HPR and GST could be effective for controlling the growth of heterogeneous human neuroblastoma cell populations.

Keywords

Apoptosis; Differentiation; N-(4-Hydroxyphenyl) retinamide; Genistein; Neuroblastoma

1. Introduction

Neuroblastoma, an embryonic tumor derived from primitive cells of the sympathetic nervous system, is the most common and deadly solid tumor in infants and children [1].

*Corresponding author. Tel.: +1-803-733-1593; fax: +1-803-733-3192. Email: swapan.ray@uscmed.sc.edu (S. K. Ray).

Amplified expression of the N-Myc proto-oncogene has been extensively correlated with highly malignant behavior and poor prognosis of neuroblastoma [2]. N-Myc expression is known to occur in 20–22% neuroblastomas and 40% of advanced cases [3] and its increased expression has been correlated with activation of genes associated with tumor aggression [4]. High N-Myc activity and low stage of neuronal differentiation have been associated with poor outcome in neuroblastoma [5]. The low stage of differentiation in neuroblastoma might also be due to the surrounding hypoxic microenvironment [6]. Hypoxic environment is known to foster the increased activity of Notch ligands and Id2 in the neural crest region resulting in low differentiation status of the neuroblastoma cells [7]. High levels of N-Myc expression without amplification in tumors has been shown to be associated with a favorable prognosis [8], and induced expression of N-Myc in p53 mutant SK-N-AS cells slows growth by increasing levels of not only apoptosis but also expression of genes to favor clinical prognosis [9].

Inactivation of tumor suppressors such as p53 might extensively contribute to inactivation of the mitotic check points resulting in steep and high cell proliferation rates [10]. Consequently, the activation of p53 results in sequence specific transcriptional activation of its downstream genes such as MDM2, Bax, and p21WAF1. Induction of p21WAF1, a cyclin-dependent kinase inhibitor, is known to induce G1 arrest until DNA has been repaired or apoptosis has been initiated [11]. Notably, p53 mutations, which are known to occur frequently in human cancers, are of rare occurrence in neuroblastoma tumors and cell lines [12]. When p53 mutations do occur they are found in progressive and relapsed neuroblastoma, suggesting that p53 mutations in neuroblastomas occur as a mechanism for resistance to cytotoxic drugs that target the p53 pathway [13]. Other aberrations in the p53 pathway occurring in neuroblastomas at relapse are MDM2 amplification and p14ARF deletion and methylation [14].

Failure of the current therapeutic regimens to inhibit N-Myc mediated angiogenic factors contributed to extensive high proliferation and invasive rates resulting in poor prognosis of neuroblastoma patients. These facts necessitated the need to develop alternative strategies using combination of different drugs. Our present study uses N-(4-hydroxyphenyl) retinamide (4-HPR), a synthetic retinoid, which effectively suppresses the growth of tumor cells [15] and also genistein (4′5,7-trihydroxyisoflavone) (GST), an isoflavanoid isolated from soybean (*Glycine max*) belonging to the family Leguminosae, which is capable of epigenetically stabilizing the expression of tumor suppressors [16] and repressing N-Myc driven growth factor mediated mitogenic cascades to induce cell cycle arrest and apoptosis. In the this study, 4-HPR promoted neuronal differentiation, while GST stabilized the expression of p53, p21, and PTEN to potentiate neuronal differentiation and induce apoptosis in human malignant neuroblastoma cells having wild type or mutant p53.

The success of any drug depends upon its efficacy in established cell lines having divergent molecular attributes. We chose two neuroblastoma cell lines SH-SY5Y and SK-N-BE2 with divergent molecular attributes. The SH-SY5Y cell line, which is a clonal variant obtained from SHSY5, contains single copy of N-Myc gene [17] and wild type p53 [18]. In contrast, the SK-N-BE2 cell line was derived from a patient with relapsed neuroblastoma harboring mutant p53 [19] and N-Myc gene amplification [20].

The present study demonstrated that combination of 4-HPR and GST suppressed the growth of both neuroblastoma cell lines by (i) down regulating the Notch1 and Id2 for repression of mesenchymal marker fibronectin to promote differentiation to neuronal phenotype, (ii) stabilizing the expression of tumor suppressors such as p53, Rb, and PTEN, and finally (iii) inducing early cell cycle exit due to G1/S phase arrest to down regulate growth factor mediated mitogenic cascade and induce apoptotic pathways in both neuroblastoma cell lines.

2. Materials and methods

2.1. Cell culture and treatments

The human malignant (N-type) neuroblastoma SH-SY5Y and SK-N-BE2 cell lines were obtained from the American Type Culture Collection (ATCC, Manassas, VA, USA). SH-SY5Y cells were maintained in 1xRPMI 1640 medium and SK-N-BE2 cells were maintained in 1xDMEM medium. Both media were supplemented with 10% fetal bovine serum (FBS) and 1% penicillin and streptomycin (GIBCO/BRL, Grand Island, NY, USA). Cell lines were maintained in a humidified atmosphere containing 5% CO_2 at 37°C. The media and FBS were purchased from Mediatech (Herndon, VA, USA). 4-HPR (Sigma Chemical, St. Louis, MO, USA) was dissolved in dimethyl sulfoxide (DMSO) to make a stock solution and stored in the dark at −70°C. To avoid light sensitivity of 4-HPR, all treatments involving it were performed under subdued lighting for 72 h. In all experiments, control cultures contained the same volume of DMSO that was used in the treatment with 4-HPR for 72 h. DMSO concentration in each experiment was always maintained at less than 0.01%, which that did not induce differentiation or cell death. Treatment of neuroblastoma cells with GST was carried out for 24 h. Following the treatments, cells were used for determination of morphological and biochemical features of neuronal differentiation or apoptosis, residual cell viability, flow cytometry, and expression of specific proteins.

2.2. Examination of morphological changes indicating induction of neuronal differentiation

Dose-response studies were conducted to optimize the concentration of 4-HPR for inducing neuronal differentiation in both neuroblastoma cell lines. Cells were cultured in monolayer in 9-cm diameter plates in the absence and presence of 0.5 μM 4-HPR for 72 h. At the end of the treatment, cells in the plates were washed twice with ice-cold phosphate-buffered saline (PBS), pH 7.4, before fixing the cells in ice-cold 95% ethanol. Cells were stained with 0.2% (v/v) methylene blue solution (prepared in 70% ethanol) for 30 s and washed twice with ice-cold de-ionized distilled water. The plates were dried in air before being examined under the light microscope at 400× magnification. The dimensions of the cells (length and width) and length of neurite were measured (n=20) using ImagePro Plus software version 4.5.1.29 (Media Cybernetics, Silver Spring, MD, USA).

2.3. Determination of residual cell viability using 3-(4,5-Dimethylthiazol-2-yl)-2,5-diphenyltetrazolium bromide (MTT) assay

All cells were grown in 6-well plates. Both SH-SY5Y and SK-N-BE2 cells were treated with 4-HPR (0.5 μM for 72 h), GST (12.5, 25, or 50 μM for 24 h), and 4-HPR (total 72 h) + GST (last 24 h). Experiments were repeated (n=3). The growth medium was supplemented with 5% FBS for the first 48 h and then replaced with fresh medium supplemented with 0.5% FBS. In case of treatment with combination, 4-HPR was still present in growth medium during the GST treatments. After the treatments, medium was discarded and replaced with a fresh medium containing MTT (0.2 mg/ml) and cells were incubated for 3 h. Then, DMSO (200 μl) was added to dissolve the MTT formazan crystals and absorbance was measured at 570 nm with background subtraction at 630 nm. Cell viability was presented as a percentage of viable cells in total population.

2.4. In situ Wright staining for detection of morphological features of apoptosis

At the completion of respective treatments, both adherent and non-adherent cells were spun down onto the microscopic slides. The cells were then washed twice with PBS, pH 7.4 before being fixed in 95% ethanol. The cells were allowed to dry before Wright staining [21]. Finally, the morphological features of the cells (n=300) were observed under the light microscope, as we described recently [21]. The morphological features of apoptotic cells

included at least one of such characteristics as cell shrinkage, chromatin condensation, and membrane-bound apoptotic bodies.

2.5. Flow cytometry for analysis of cell cycle and apoptosis

Cells were harvested at the completion of the respective treatments (n=3) and washed with PBS (pH 7.4) twice before being fixed with 70% ethyl alcohol for 15 min on ice. Subsequently, the cells were centrifuged at a low rpm to obtain pellets and residual alcohol was aspirated. Cells were then digested with DNase-free RNase A (2 mg/ml) for 30 min at 37°C. Before flow cytometric analysis, cells were resuspened in 1 ml of 10 μg/ml propidium iodide (PI) (Sigma-Aldrich, St. Louis, MO, USA) for staining cellular DNA, as we described recently [22]. Cellular DNA content was then analyzed using an Epics XL-MCL Flow Cytometer (Beckman Coulter, Fullerton, CA, USA). The cell cycle results were analyzed for statistical significance. For Annexin V staining, the cells were treated (n=3), harvested, and washed with PBS (pH 7.4) twice, processed as per the manufacturer's instructions (Vybrant Apoptosis Assay Kit, Molecular Probes, Eugene, OR, USA), and then analyzed on Epics XL-MCL Flow Cytometer (Beckman Coulter). The Annexin V staining results were analyzed for statistical significance.

2.6. Antibodies and Western blotting

Monoclonal antibody against β-actin (clone AC-15) was purchased (Sigma-Aldrich, St. Louis, MO, USA) and used to monitor the equal loading of cytosolic proteins on sodium dodecyl sulfate-polyacrylamide gels (SDS-PAGE) experiments, as we described previously [23]. Both the neuroblastoma SH-SY5Y and SK-N-BE2 cell lines were treated with 4-HPR (72 h) and GST (24 h) alone and in combination prior to extraction of protein samples. Protein samples obtained from neuroblastoma cells were resoled on the SDS-PAGE gels and analyzed by Western blotting using the primary IgG antibodies against p-Akt (Thr 308), Bax, Bcl-2, Bid, caspase-3, caspase-8, CDK2, e-cadherin, E2F1, EGFR, 42/44 Erk1/2, fibronectin, b-FGF, Hes-1, ICAD, Id2, MAD2, MMP-2, MMP-9, p65 NF-κB, Notch-1, N-Myc, p21, acetyl-p53, p53, PCNA, PTEN, retinoblastoma (Rb), p-Rb (Ser 780), survivin, hTERT, and VEGF. Primary IgG antibodies against all proteins with the exception of fibronectin were procured from Santa Cruz Biotechnology (Santa Cruz, CA, USA). Primary IgG antibody against fibronectin (IST 9) was obtained from Abcam (Cambridge, MA, USA). The horseradish peroxidase conjugated goat anti-mouse or anti-rabbit secondary IgG antibody (ICN Biomedicals, Aurora, OH, USA) was used. Western blots were incubated with enhanced chemiluminescence (ECL) detection reagents (Amersham Pharmacia, Buckinghamshire, UK) and exposed to X-OMAT AR films (Eastman Kodak, Rochester, NY, USA) for autoradiography. The autoradiograms were scanned on an EPSON Scanner using Photoshop software (Adobe Systems, Seattle, WA, USA) and optical density (OD) of each band was determined using the NIH Image software. The OD of bands in the control treatment was designated as 100. All experiments were performed in triplicates and results were analyzed for statistical significance.

2.7. Statistical analysis

Results were analyzed using StatView software (Abacus Concepts, Berkeley, CA, USA) and compared using one-way analysis of variance (ANOVA) with Fisher's post hoc test. Data were presented as mean ± standard error of mean (SEM) of separate experiments ($n \geq 3$). Significant difference from control value was indicated by $^{*}P < 0.05$, $^{**}P < 0.005$, or $^{\#}P < 0.001$.

3. Results

3.1. Morphological and biochemical features of 4-HPR induced neuronal differentiation in SH-SY5Y and SK-N-BE2 cells

Treatment with 0.5 μM 4-HPR for 72 h induced neuronal differentiation in both SH-SY5Y and SK-N-BE2 cell lines (Fig. 1). The morphological features of neuronal differentiation were assessed following *in situ* methylene blue staining (Fig. 1A). Microscopic observations (n=20) revealed that 4-HPR treatment induced small and retracted cell bodies having thin elongated and branched neurite extensions, while the untreated (control) neuroblastoma cells maintained wide cell body with short cytoplasmic processes. The measurements of morphological features confirmed that length of the cell and neurite extensions were significantly increased in 4-HPR treated cells, compared with control cells (Fig. 1B). Many signaling molecules [N-Myc, Notch-1, Id2, Hes-1, fibronectin, catalytic subunit of human telomerase (hTERT), and proliferation cell nuclear antigen (PCNA)] associated with neuronal dedifferentiation were decreased significantly following treatment with combination of 4-HPR (total 72 h) and GST (last 24 h) in both cell lines (Fig. 1C and Supplementary Fig. 1C). Differentiation in neuroblastoma cells was evidenced by not only alterations in cell morphology but also by increased expression of the tight junction protein e-cadherin, especially after the combination therapy (Fig. 1C and Supplementary Fig. 1C). Notably, 4-HPR alone and also in combination with GST increased expression of tight junction protein e-cadherin. Induction of neuronal differentiation by the combination of 4-HPR and GST greatly decreased the expression of hTERT and PCNA leading to inhibition of cell proliferation.

3.2. Combination of 4-HPR and GST reduced viability of neuroblastoma cell lines

We determined the changes in residual cell viability of neuroblastoma SH-SY5Y and SK-N-BE2 cells after treatment with 4-HPR (0.5 μM for 72 h), GST (12.5, 25, or 50 μM for 24 h), and 4-HPR (total 72 h) + GST (last 24 h) using the MTT assay (Fig. 2). To state more clearly, we treated the cells first with 0.5 μM 4-HPR for 48 h and then added 12.5, 25, or 50 μM GST to the culture to continue the co-treatment for next 24 h. The MTT assay revealed that although 0.5 μM 4-HPR alone did not induce any significant decrease in cell viability, treatment with 25 and 50 μM GST alone and combination of 4-HPR and GST (25 or 50 μM) significantly reduced the cell viability in both neuroblastoma cell lines. In all subsequent experiments, we used 0.5 μM 4-HPR + 25 μM GST as an effective combination for inducing cell death in neuroblastoma cells and examining the alterations in molecular markers that led to this process.

3.3. Combination of 4-HPR and GST induced cell cycle arrest at G1/S phase due to stabilization of tumor suppressors

Combination of 4-HPR and GST caused cell cycle arrest at G1/S phase with alterations in the levels of key signaling molecules governing the G1/S phase mitotic check point (Fig. 3). Flow cytometric analysis of the propidium iodide (PI) stained cells following the treatments revealed substantial alterations in the distribution of cells in different phases of cell cycle (Fig. 3A and Supplementary Fig. 3A). Treatment of SH-SY5Y cells with 4-HPR alone did not dramatically alter populations in the G0/G1 and G2/M phases (Supplementary Fig. 3A). In contrast, alterations were observed in the distribution of cells in the G0/G1 and G2/M phases in SK-N-BE2 cells after treatment with 4-HPR (Supplementary Fig. 3A). Treatment of cells with GST alone substantially increased populations in G0/G1 phase. Interestingly, combination of 4-HPR and GST very significantly increased distribution of cells in the G0/G1 phase in both cell lines (Fig. 3A and Supplementary Fig. 3A). Results suggested that combination of 4-HPR and GST worked co-operatively to impose an early cell cycle exit due to arrest at G1/S phase of the cell cycle.

Western blotting indicated that induction of cell cycle arrest at G1/S phase was correlated with changes in levels of key signaling molecules governing the G1/S mitotic check point (Fig. 3B). Acetylation of non-histone proteins such as p53 (tumor suppressor protein) is known to contribute to increased stability of the G1/S mitotic check point [24]. Combination of 4-HPR and GST increased the acetylation of p53 at Lys 382 residue to enhance its stability and upregulated p21 and Rb (tumor suppressor protein) in both neuroblastoma cell lines (Fig. 3B and Supplementary Fig. 3B). Treatment of cells with combination of 4-HPR and GST triggered the events to decrease the S phase products thereby inducing an inhibition on cell proliferation, contributing to cell cycle arrest at G1/S phase.

Appearance of mitotic abnormalities is a key event to contribute to cell cycle arrest. Combination of 4-HPR and GST caused down regulation of CDK2 and E2F1 and also sustained reduction in the levels of mitotic arrest deficient 2 (MAD2) and survivin in both SH-SY5Y and SK-N-BE2 cells (Fig. 3B and Supplementary Fig. 3B). Cellular down regulation of the keystone mitotic molecules (CDK2, E2F1, MAD2, and survivin) in response to treatment with combination of 4-HPR and GST contributed extensively to the cell cycle arrest at G1/S phase.

3.4. Induction of morphological and biochemical features of apoptosis

The onset of cell cycle arrest was accompanied by appearance of morphological and biochemical features of apoptosis, as we examined using *in situ* Wright staining and flow cytometric analysis (Fig. 4). *In situ* Wright staining showed the morphological changes in apoptotic cells (Fig. 4A). Characteristic morphological features of apoptotic cells included shrinkage of cell volume, chromatin condensation, and membrane-bound apoptotic bodies that appeared prominently following treatment of cells with combination of 4-HPR and GST (Fig. 4A). *In situ* Wright staining was used for counting the cells (n=300) and determining the amounts of apoptosis (Fig. 4B). Treatment of cells with 4-HPR alone showed a marginal increase in the percentage of apoptotic cells. In contrast, treatment of cells with GST alone or a combination of 4-HPR and GST showed significant increase in the percentage of apoptosis in both SH-SY5Y and SK-N-BE2 cells (Fig. 4B). These results were further substantiated by the flow cytometric analysis of Annexin V positive cells (Fig. 4C). An increase in population of Annexin V positive cells in A4 area indicated occurrence of apoptosis, as shown in both SH-SY5Y and SK-N-BE2 cells following treatment with combination of 4-HPR and GST (Fig. 4C). Based on flow cytometric analysis of Annexin V positive cells, we determined the percentages of apoptosis in SH-SY5Y and SK-N-BE2 cells after the treatments (Fig. 4D). Compared with control SH-SY5Y or SK-N-BE2 cells, treatment with 4-HPR alone did not increase the number of Annexin V positive cells but treatment with GST alone significantly increased the population of Annexin V positive cells (Fig. 4D). Treatment with combination of 4-HPR and GST very significantly increased the percentages of the Annexin V positive populations in both SH-SY5Y and SK-N-BE2 cells (Fig. 4D). The increase in Annexin V positive cells after the treatment was a prominent biochemical feature of apoptosis in neuroblastoma cells.

3.5. Cell cycle arrest repressed growth factor and mitogenic signaling cascade

One of the salient observations made in the present study was the incremental expression of the tumor suppressor PTEN in response to GST alone and combination of 4-HPR and GST in both SH-SY5Y and SK-N-BE2 cells (Fig. 5 and Supplementary Fig. 5). N-Myc mediated oncogenic signaling plays a significant role in clinical pathogenesis of neuroblastoma. Increase in expression of PTEN is known to be associated with repression of N-Myc driven angiogenic and growth factors. Following combination therapy, prominent increase in expression of PTEN correlated well with suppression of expression of angiogenic factors (VEGF and b-FGF), growth factor receptor (EGFR), and invasive factors such as matrix

metalloproteinases (MMP-2 and MMP-9) in both neuroblastoma cells (Fig. 5 and Supplementary Fig. 5). Overexpression of the tumor suppressor is also known to suppress activation (phosphorylation) of Akt and down regulate Erk 1/2 and NF-κB survival pathways. Our Western blotting demonstrated that combination of 4-HPR and GST effectively upregulated PTEN and down regulated phosphorylation of Akt (Thr 308) and suppressed NF-κB and Erk 1/2 (Fig. 5 and Supplementary Fig. 5). Thus, combination of 4-HPR and GST was highly efficient in upregulating PTEN and down regulating angiogenic factors, survival pathways, and mitogenic cascade to facilitate cell cycle arrest and apoptosis in neuroblastoma cells.

3.6. Combination of 4-HPR and GST activated extrinsic and intrinsic apoptotic cascades

Morphological features of apoptosis induced by treatment with combination of 4-HPR and GST were correlated with the expression of key signaling molecules involved in the activation of both extrinsic and intrinsic pathways to increase proteolytic activities for apoptosis (Fig. 6 and Supplementary Fig. 6). Our results showed activation of extrinsic apoptotic pathway in increases in generation of active caspase-8 in both SH-SY5Y and SK-N-BE2 cells following treatment with GST alone and also combination of 4-HPR and GST. Activation of caspase-8 cleaved 22 kD Bid to generate 15 kD truncated Bid (tBid), which could translocate to mitochondria to induce the release of cytochrome c for activating mitochondrial apoptotic pathway [25]. Moreover, migration of cytoplasmic protein Bax to mitochondria could cooperate with tBid to release cytochrome c [26]. We found prominent increases in proteolytic cleavage of Bid to tBid in cells treated with GST alone and also after treatment with combination of 4-HPR and GST (Fig. 6 and Supplementary Fig. 6). Further, combination of 4-HPR and GST induced intrinsic apoptotic pathway as evidenced from an increase in expression of Bax (pro-apoptotic protein) and decrease in expression of Bcl-2 (anti-apoptotic protein), resulting in an increase in Bax:Bcl-2 ratio in both cell lines (Fig. 6 and Supplementary Fig. 6). The polyclonal antibody used in this investigation could recognize only 23 kD Bax. The increase in Bax:Bcl-2 ratio is known to alter mitochondrial permeability to release cytochrome c into the cytosol, triggering activation of intrinsic apoptotic cascade. Cytosolic protein Apaf1 and cytochrome c participate in caspase-9-dependent activation of caspase-3 [27]. Upon activation, caspase-3 could activate and release caspase-activated DNase (CAD) by cleaving and inactivating the inhibitor of caspase-activated DNase (ICAD). Combination of 4-HPR and GST very efficiently caused activation of caspase-3 and cleavage of ICAD in both cell lines (Fig. 6 and Supplementary Fig. 6).

Based on the results from our investigation, we outlined schematic pathways showing molecular events that induced neuronal differentiation as well as apoptotic cascades following treatment of neuroblastoma cells with combination of 4-HPR and GST (Fig. 7). We propose that combination of 4-HPR and GST induced neuronal differentiation in both SH-SY5Y and SK-N-BE2 cells along with decreased expression of markers of dedifferentiation (N-Myc, Notch-1, Id2, and hTERT). This transition to neuronal phenotype was accompanied by increased level of e-cadherin and reduced level of the mesenchymal marker fibronectin. Combination of 4-HPR and GST activated the expression of multiple tumor suppressors, which acted in concert to induce cell cycle arrest at G1/S phase. The induction of G1/S phase cell cycle arrest resulted in mitotic abnormalities. Together all the events significantly contributed to repression of N-Myc driven angiogenic and growth factors resulting in down regulation of survival pathways and mitogenic cascade. These changes in molecular events induced the activation of intrinsic and extrinsic apoptotic pathways.

4. Discussion

The results obtained from this investigation show that combination of 4-HPR and GST down regulated N-Myc directed dedifferentiation factors to effectively induce differentiation to neuronal phenotype in human malignant neuroblastoma SH-SY5Y (wild type p53) and SK-N-BE2 (mutant p53) cells. Transition to neuronal phenotype was accompanied by increased expression of the tight junction protein e-cadherin along with decreased levels of fibronectin, hTERT, and PCNA. We report for the first time that combination of 4-HPR and GST induced early cell cycle exit due to G1/S phase arrest in two neuroblastoma cell lines to induce the reactivation of multiple tumor suppressors (p53, p21, Rb, and PTEN). Reactivation of these tumor suppressors led to the suppression of N-Myc mediated angiogenic factors (VEGF and b-FGF) and invasive factors (MMP-2 and MMP-9), resulting in repression of components of the survival and mitogenic pathways [p-Akt (Thr 308), p65 NF-κB, and p42/44 Erk 1/2]. Taken together, combination of 4-HPR and GST effectively blocked the angiogenic and survival advantages in two different neuroblastoma cell lines leading to induction of apoptosis, suggesting that this combination of drugs could be used as an effective strategy for controlling the growth of heterogeneous populations of neuroblastoma.

Retinoids have been extensively used along with the histone deacetylase (HDAC) inhibitors to induce differentiation in neuroblastoma cells [28]. In fact, 4-HPR has been used in several carcinomas to induce cellular differentiation [29] due to its low toxicity profile and anti-proliferative activities [30]. As we found in this investigation, a low dose of 4-HPR (0.5 μM) induced neuronal differentiation resulting in reduced width of the cell along with significant increase in the length of the cell as well as neurite extensions (Fig. 1). Transformation to neuronal phenotype was accompanied by substantial decrease in the levels of N-Myc and its downstream targets Notch-1 and Id2, which were shown to promote dedifferentiation of neuroblastoma cells under hypoxic conditions [6]. This was also accompanied by repression in the levels of fibronectin (a marker for mesenchymal transition) [31], whose overexpression contributes to the poor prognosis in several cancers [32,33]. Induction of neuronal phenotype was correlated with repression of cell proliferation markers such as PCNA, hTERT, and E2F1. To our knowledge, this is the first report correlating the repression of N-Myc and its downstream targets Notch1 and Id2 with the onset of 4-HPR mediated neuronal differentiation in two neuroblastoma cell lines harboring differential levels of N-Myc. Treatment with GST (25 μM) significantly down regulated the viability of differentiated cells in both the cell lines (Fig. 2)

Flow cytometric analyses revealed that combination of 4-HPR and GST induced early cell cycle exit (Fig. 3) for induction of apoptosis (Fig. 4) in neuroblastoma cells. These are significant observations as higher concentrations of GST usually result in G2/M phase arrest [34,35]. Earlier reports also suggest that neuronal differentiation is associated with loss of multi-potency resulting in irreversible early cell cycle exit [36]. Lower concentrations of GST have been recently shown to induce maximum accumulation of cells in the G0/G1 phase without inducing G2/M phase arrest [37].

We observed reactivation of multiple tumor suppressors (p53, p21, Rb, and PTEN) in response to treatment of neuroblastoma cells with combination of 4-HPR and GST (Figs. 3 and 5). Reactivation of the p53 pathway in SK-N-BE2 cell line is of clinical importance as this cell line harbors mutant p53. Hyperacetylation of p53 at Lys 382 residue increased its stability in both SH-SY5Y and SK-N-BE2 cell lines (Fig. 3). Reactivation of p53 pathway has previously been shown in these cell lines in response to low concentration of HDAC inhibitors [38]. We also observed that downstream targets of p53 pathway (p21, Bax, and caspase-3) were also upregulated in neuroblastoma cells following treatment with

combination of 4-HPR and GST (Figs. 3 and 6). The tumor suppressor p53 exerts its effect on the cell cycle by upregulating the expression of its downstream tumor suppressor p21. Increased expression of p21 repressed the mitogenic signaling of G1 phase cyclins by down regulating the expression of CDK2 (Fig. 3). This in turn enhanced the stability of the tumor suppressor Rb by its dephosphorylation at Ser 780 residue in both the cell lines (Fig. 3). Hypophosphorylation of Rb repressed the expression of E2F1 (Fig. 3), the transcriptional factor known to be associated with high risk neuroblastomas [39]. Also, E2F1 suppresses MAD2 as well as survivin resulting in loss of anaphase promoting complex activity [40], thereby contributing to cell cycle arrest at G1/S phase. Our results showed that combination of 4-HPR and GST enhanced the stability of Rb, which in turn repressed E2F1, MAD2, and survivin to differential levels resulting in cell cycle arrest (Fig. 3). Combination of 4-HPR and GST induced differential amounts of apoptosis in both neuroblastoma cell lines (Fig. 4).

N-Myc driven growth factor mediated mitogenic pathways contribute significantly to the growth and invasiveness of neuroblastoma [41]. N-Myc induces angiogenesis in the surrounding microenvironment due to activation of pro-angiogenic growth factors such as VEGF and b-FGF and also invasive factors such as matrix metalloproteinases [42]. We showed that combination of 4-HPR and GST very efficiently down regulated both angiogenic (VEGF and b-FGF) and invasive (MMP-2 and MMP-9) factors in both neuroblastoma cells lines (Fig. 5). These findings are particularly significant, as one of the cell lines used in the present study (SK-N-BE2) has N-Myc amplification.

N-Myc driven growth factor mediated mitogenic cascade is activated through the mitogen activated protein kinase and PI3K/Akt survival pathways, which collectively control cellular differentiation, proliferation, and apoptosis. These pathways harbor the ability to amplify cellular proliferation and inhibit apoptosis as well as influence the downstream NF-κB pathway [43,44]. GST has been shown to activate PTEN through epigenetic remodeling [16]. PTEN negatively regulates PI3K/Akt pathway by dephosphorylating phosphatidylinositol-3,4,5-triphosphate [45]. We found that combination of 4-HPR and GST upregulated PTEN to inhibit components of N-Myc driven growth factor mediated angiogenic and survival (VEGF, b-FGF, EGFR, MMP-2, MMP-9, p-Akt, NF-κB, and Erk 1/2) pathways (Fig. 6). Down regulation of these pathways are particularly important from the clinical perspective as neuroblastomas harboring amplification of N-Myc are more resistant to chemotherapy.

In conclusion, reduction in N-Myc expression and induction of cell cycle arrest at G1/S phase following treatment with combination of 4-HPR and GST resulted in significant increase in morphological and biochemical features of apoptosis. We analyzed some of the components of the extrinsic and intrinsic pathways of apoptosis. Combination of 4-HPR and GST activated extrinsic pathway of apoptosis with activation of caspase-8 followed by cleavage of Bid to tBid. In addition to generation of tBid, overexpression of the pro-apoptotic protein Bax potentiated activation of intrinsic pathway of apoptosis. These events led to the activation of the effector caspase-3, which in turn cleaved ICAD to release CAD for its translocation to the nucleus for degradation of genomic DNA, the final event in apoptosis.

Supplementary Material

Refer to Web version on PubMed Central for supplementary material.

Acknowledgments

This work was supported in part by the R01 grants (NS-57811 and CA-91460) from the National Institutes of Health (Bethesda, MD, USA).

References

1. Brodeur GM. Neuroblastoma: biological insights into a clinical enigma. Nat Rev Cancer. 2003; 3:203–16. [PubMed: 12612655]
2. Schwab M. MYCN in neuronal tumours. Cancer Lett. 2004; 204:179–87. [PubMed: 15013217]
3. Cohn SL, Tweddle DA. MYCN amplification remains prognostically strong 20 years after its "clinical debut". Eur J Cancer. 2004; 40:2639–42. [PubMed: 15571946]
4. Norris MD, Bordow SB, Marshall GM, Haber PS, Cohn SL, Haber M. Expression of the gene for multidrug-resistance-associated protein and outcome in patients with neuroblastoma. N Engl J Med. 1996; 334:231–8. [PubMed: 8532000]
5. Fredlund E, Ringner M, Maris JM, Pahlman S. High Myc pathway activity and low stage of neuronal differentiation associate with poor outcome in neuroblastoma. Proc Natl Acad Sci USA. 2008; 105:14094–9. [PubMed: 18780787]
6. Jogi A, Ora I, Nilsson H, Lindeheim A, Makino Y, Poellinger L, et al. Hypoxia alters gene expression in human neuroblastoma cells toward an immature and neural crest-like phenotype. Proc Natl Acad Sci U S A. 2002; 99:7021–6. [PubMed: 12011461]
7. Löfstedt T, Jögi A, Sigvardsson M, Gradin K, Poellinger L, Pahlman S, et al. Induction of ID2 expression by hypoxia-inducible factor-1: a role in dedifferentiation of hypoxic neuroblastoma cells. J Biol Chem. 2004; 279:39223–31. [PubMed: 15252039]
8. Tang XX, Robinson ME, Riceberg JS, Kim DY, Kung B, Titus TB, et al. Favorable neuroblastoma genes and molecular therapeutics of neuroblastoma. Clin Cancer Res. 2004; 10:5837–44. [PubMed: 15355914]
9. Tang XX, Zhao H, Kung B, Kim DY, Hicks SL, Cohn SL, et al. The MYCN enigma: significance of MYCN expression in neuroblastoma. Cancer Res. 2006; 66:2826–33. [PubMed: 16510605]
10. Hollstein M, Sidransky D, Vogelstein B, Harris CC. p53 mutations in human cancers. Science. 1991; 253:49–53. [PubMed: 1905840]
11. Vogelstein B, Lane D, Levine AJ. Surfing the p53 network. Nature. 2000; 408:307–10. [PubMed: 11099028]
12. Keshelava N, Zuo JJ, Waidyaratne NS, Triche TJ, Reynolds CP. p53 mutations and loss of p53 function confer multidrug resistance in neuroblastoma. Med Pediatr Oncol. 2000; 35:563–8. [PubMed: 11107118]
13. Tweddle DA, Pearson AD, Haber M, Norris MD, Xue C, Flemming C, et al. The p53 pathway and its inactivation in neuroblastoma. Cancer Lett. 2003; 197:93–8. [PubMed: 12880966]
14. Carr J, Bell E, Pearson AD, Kees UR, Beris H, Lunec J, et al. Increased frequency of aberrations in the p53/MDM2/p14(ARF) pathway in neuroblastoma cell lines established at relapse. Cancer Res. 2006; 66:2138–45. [PubMed: 16489014]
15. Sabichi AL, Hendricks DT, Bober MA, Birrer MJ. Retinoic acid receptor beta expression and growth inhibition of gynecologic cancer cells by the synthetic retinoid N-(4-hydroxyphenyl) retinamide. J Natl Cancer Inst. 1998; 90:597–605. [PubMed: 9554442]
16. Kikuno N, Shiina H, Urakami S, Kawamoto K, Hirata H, Tanaka Y, et al. Genistein mediated histone acetylation and demethylation activates tumor suppressor genes in prostate cancer cells. Int J Cancer. 2008; 123:552–60. [PubMed: 18431742]
17. Feng X, Jiang H, Baik JC, Edgar C, Eide FF. BDNF dependence in neuroblastoma. J Neurosci Res. 2001; 64:355–63. [PubMed: 11340642]
18. Davidoff AM, Pence JC, Shorter NA, Iglehart JD, Marks JR. Expression of p53 in human neuroblastoma- and neuroepithelioma-derived cell lines. Oncogene. 1992; 7:127–33. [PubMed: 1741160]
19. Tweddle DA, Malcolm AJ, Cole M, Pearson AD, Lunec J. p53 cellular localization and function in neuroblastoma: evidence for defective G1 arrest despite WAF1 induction in MYCN-amplified cells. Am J Pathol. 2001; 158:2067–77. [PubMed: 11395384]
20. Gabriele B, Enrico T. BDNF splice variants from the second promoter cluster support cell survival of differentiated neuroblastoma upon cytotoxic stress. J Cell Sci. 2009; 122:36–43. [PubMed: 19050044]

21. Janardhanan R, Banik NL, Ray SK. N-(4-Hydroxyphenyl) retinamide induced differentiation with repression of telomerase and cell cycle to increase interferon-gamma sensitivity for apoptosis in human glioblastoma cells. Cancer Lett. 2008; 261:26–36. [PubMed: 18164543]
22. Janardhanan R, Butler JT, Banik NL, Ray SK. N-(4-Hydroxyphenyl) retinamide potentiated paclitaxel for cell cycle arrest and apoptosis in glioblastoma C6 and RG2 cells. Brain Res. 2009; 1268:142–53. [PubMed: 19285047]
23. Ray SK, Karmakar S, Nowak MW, Banik NL. Inhibition of calpain and caspase-3 prevented apoptosis and preserved electrophysiological properties of voltage-gated and ligand-gated ion channels in rat primary cortical neurons exposed to glutamate. Neuroscience. 2006; 139:577–95. [PubMed: 16504408]
24. Glozak MA, Sengupta N, Zhang X, Seto E. Acetylation and deacetylation of non-histone proteins. Gene. 2005; 363:15–23. [PubMed: 16289629]
25. Luo X, Budihardjo I, Zou H, Slaughter C, Wang X. Bid, a Bcl2 interacting protein, mediates cytochrome c release from mitochondria in response to activation of cell surface death receptors. Cell. 1998; 94:481–90. [PubMed: 9727491]
26. Murphy KM, Streips UN, Lock RB. Bax membrane insertion during Fas(CD95)-induced apoptosis precedes cytochrome c release and is inhibited by Bcl-2. Oncogene. 1999; 18:5991–9. [PubMed: 10557088]
27. Saleh A, Srinivasula SM, Acharya S, Fishel R, Alnemri ES. Cytochrome c and dATP-mediated oligomerization of Apaf-1 is a prerequisite for procaspase-9 activation. J Biol Chem. 1999; 274:17941–5. [PubMed: 10364241]
28. De los Santos M, Zambrano A, Aranda A. Combined effects of retinoic acid and histone deacetylase inhibitors on human neuroblastoma SH-SY5Y cells. Mol Cancer Ther. 2007; 6:1425–32. [PubMed: 17431121]
29. Naik HR, Kalemkerian G, Pienta KJ. 4-Hydroxyphenylretinamide in the chemoprevention of cancer. Adv Pharmacol. 1995; 33:315–47. [PubMed: 7495674]
30. Veronesi U, Mariani L, Decensi A, Formelli F, Camerini T, Miceli R, et al. Fifteen-year results of a randomized phase III trial of fenretinide to prevent second breast cancer. Ann Oncol. 2006; 17:1065–71. [PubMed: 16675486]
31. Thiery JP. Epithelial-mesenchymal transitions in development and pathologies. Curr Opin Cell Biol. 2003; 15:740–6. [PubMed: 14644200]
32. Yauch RL, Januario T, Eberhard DA, Cavet G, Zhu W, Fu L, et al. Epithelial versus mesenchymal phenotype determines in vitro sensitivity and predicts clinical activity of erlotinib in lung cancer patients. Clin Cancer Res. 2005; 11:8686–98. [PubMed: 16361555]
33. Xu J, Wang R, Xie ZH, Odero-Marah V, Pathak S, Multani A, et al. Prostate cancer metastasis: role of the host microenvironment in promoting epithelial to mesenchymal transition and increased bone and adrenal gland metastasis. Prostate. 2006; 66:1664–73. [PubMed: 16902972]
34. Ismail IA, Kang KS, Lee HA, Kim JW, Sohn YK. Genistein-induced neuronal apoptosis and G2/M cell cycle arrest is associated with MDC1 upregulation and PLK1 down regulation. Eur J Pharmacol. 2007; 575:12–20. [PubMed: 17706963]
35. Rauth S, Kichina J, Green A. Inhibition of growth and induction of differentiation of metastatic melanoma cells in vitro by genistein: chemosensitivity is regulated by cellular p53. Br J Cancer. 1997; 75:1559–66. [PubMed: 9184169]
36. Kuzumaki T, Kobayashi T, Ishikawa K. Genistein induces p21(Cip1/WAF1) expression and blocks the G1 to S phase transition in mouse fibroblast and melanoma cells. Biochem Biophys Res Commun. 1998; 251:291–5. [PubMed: 9790949]
37. Alvarez-Rodriguez R, Pons S. Expression of the proneural gene encoding Mash1 suppresses MYCN mitotic activity. J Cell Sci. 2009; 122:595–9. [PubMed: 19208763]
38. Condorelli F, Gnemmi I, Vallario A, Genazzani AA, Canonico PL. Inhibitors of histone deacetylase (HDAC) restore the p53 pathway in neuroblastoma cells. Br J Pharmacol. 2008; 153:657–68. [PubMed: 18059320]
39. Hernando E, Nahle Z, Juan G, Diaz-Rodriguez E, Alaminos M, Hemann M, et al. Rb inactivation promotes genomic instability by uncoupling cell cycle progression from mitotic control. Nature. 2004; 430:797–802. [PubMed: 15306814]

40. Cleveland DW, Mao Y, Sullivan KF. Centromeres and kinetochores: from epigenetics to mitotic checkpoint signaling. Cell. 2003; 112:407–21. [PubMed: 12600307]
41. Misawa A, Hosoi H, Arimoto A, Shikata T, Akioka S, Matsumura T, et al. N-Myc induction stimulated by insulin-like growth factor I through mitogen-activated protein kinase signaling pathway in human neuroblastoma cells. Cancer Res. 2000; 60:64–9. [PubMed: 10646854]
42. Chesler L, Goldenberg DD, Seales IT, Satchi-Fainaro R, Grimmer M, Collins R, et al. Malignant progression and blockade of angiogenesis in a murine transgenic model of neuroblastoma. Cancer Res. 2007; 67:9435–42. [PubMed: 17909053]
43. Martin V, Herrera F, Garcia-Santos G, Antolin I, Rodriguez-Blanco J, Rodriguez C. Signaling pathways involved in antioxidant control of glioma cell proliferation. Free Radic Biol Med. 2007; 42:1715–22. [PubMed: 17462539]
44. Karin M, Cao Y, Greten FR, Li ZW. NF-κB in cancer: from innocent bystander to major culprit. Nat Rev Cancer. 2002; 2:301–10. [PubMed: 12001991]
45. Stambolic V, Suzuki A, de la Pompa JL, Brothers GM, Mirtsos C, Sasaki T, et al. Negative regulation of PKB/Akt-dependent cell survival by the tumor suppressor PTEN. Cell. 1998; 95:29–39. [PubMed: 9778245]

Appendix A. Supplementary data

Supplementary data associated with this investigation can be found in the online version of this article.

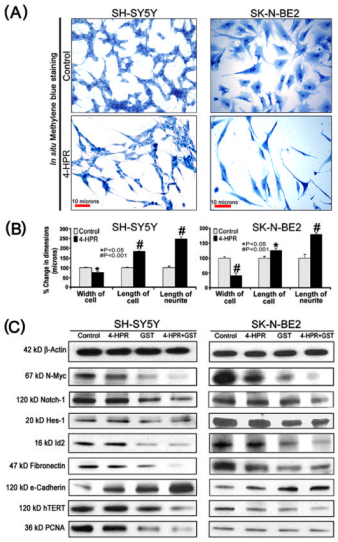

Fig. 1.

Treatment with 4-HPR decreased cell proliferation and induced morphological and biochemical features of neuronal differentiation. (A) Decrease in cell proliferation and increase in morphological features of neuronal differentiation. Cells were treated with 0.5 μM 4-HPR for 72 h. Appearance of morphological features of neuronal differentiation included small, thin, and retracted cell bodies with elongated and branched processes. (B) Measurement of dimensions of neuronal differentiation (width of cell, length of cell, and length of neurite extension). Treatment of cells with 4-HPR produced significant differences in all these attributes measured. The length of cell and the neurite extensions were significantly increased due to neuronal differentiation, when compared with control cells. A concomitant decrease in the width of cell was observed following treatment with 4-HPR. (C) Representative Western blots to show changes in biochemical markers of neuronal differentiation and cell proliferation. Treatments: control, 0.5 μM 4-HPR for 72 h, 25 μM GST for 24 h, and 0.5 μM 4-HPR for 48 h (pretreatment) + 25 μM GST for 24 h. Expression of β-actin was used as a loading control. All experiments were conducted in triplicates.

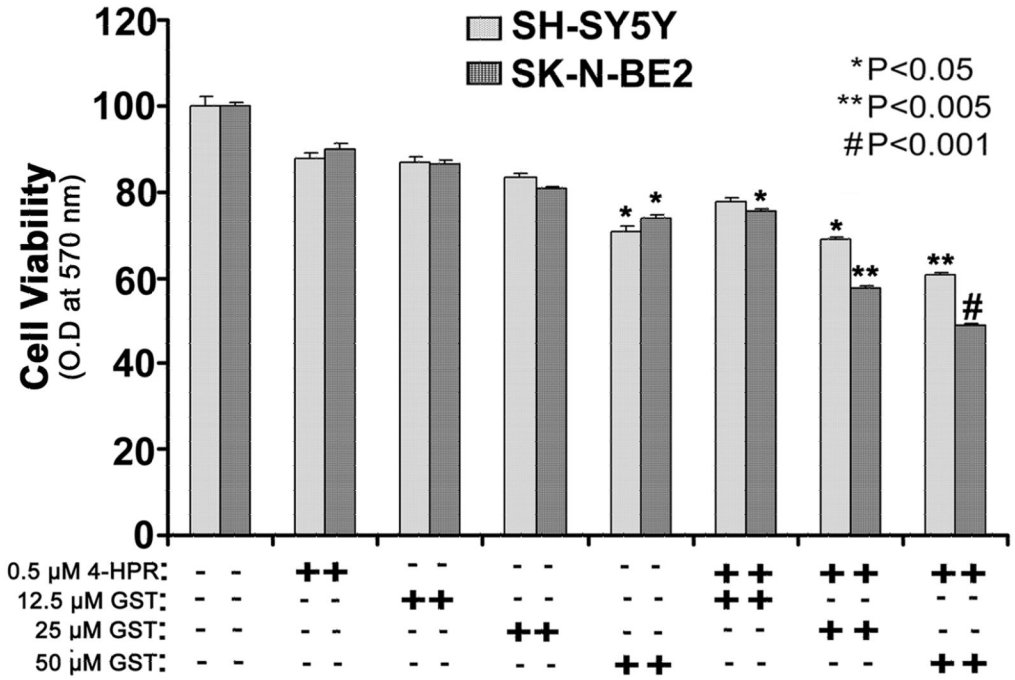

Fig. 2.

Changes in residual cell viability following the treatments. Cells were treated with 4-HPR for 72 h, GST for 24 h, and also pretreated with 4-HPR for 48 h and then treated with GST for 24 h. After the treatments, changes in cell viability were determined by the MTT assay. All experiments were conducted in triplicates and the results were analyzed for statistical significance.

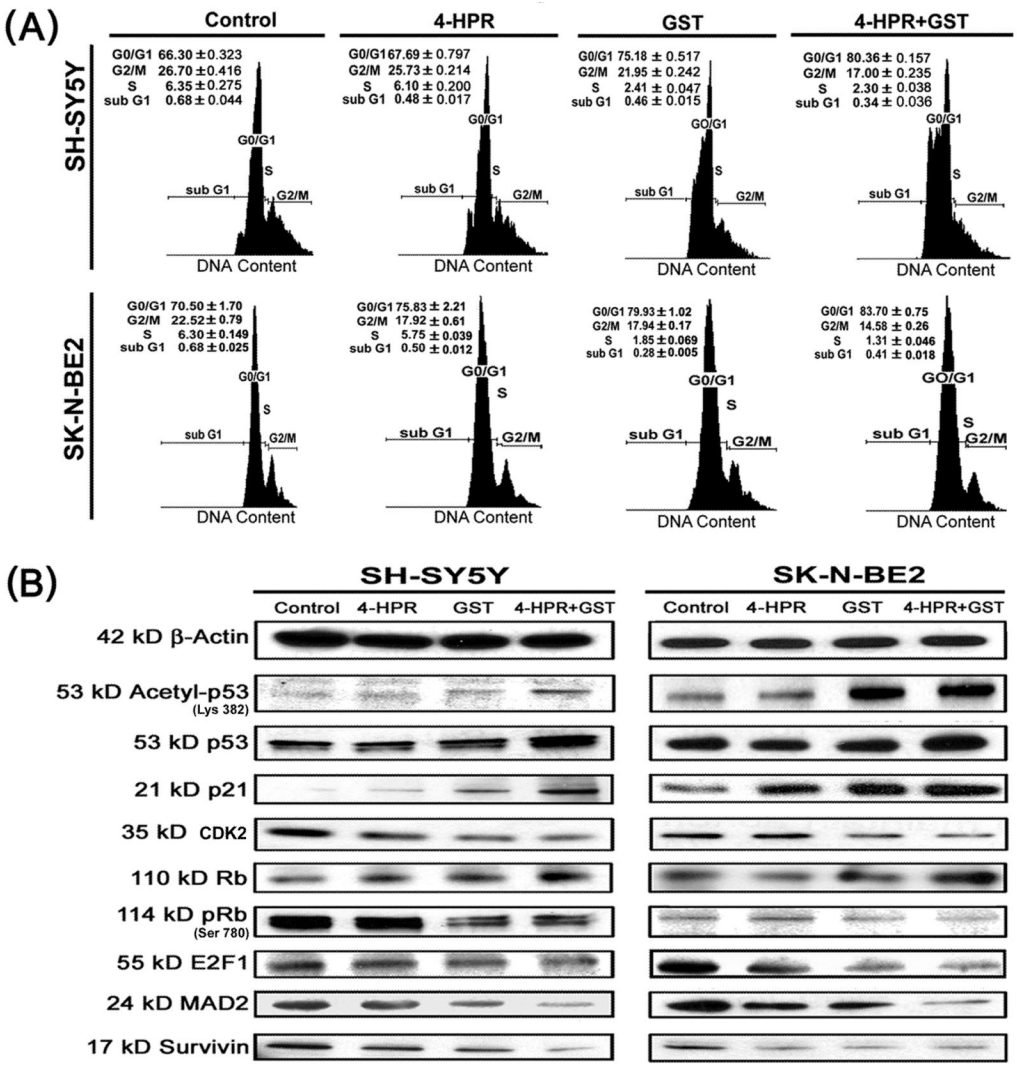

Fig. 3.

Cell cycle analysis and changes in levels of molecules governing the cell cycle. Treatments: control, 0.5 μM 4-HPR for 72 h, 25 μM GST for 24 h, and 0.5 μM 4-HPR for 48 h (pretreatment) + 25 μM GST for 24 h. (A) Flow cytometric analysis of cell cycle. Distributions of cells in the G0/G1, G2/M, S, and sub G1 phases were analyzed. (B) Representative Western blots to show changes in cytosolic levels of molecular markers associated with cell cycle arrest at G1/S phase. Expression of β-actin was used as a loading control. All experiments were conducted in triplicates.

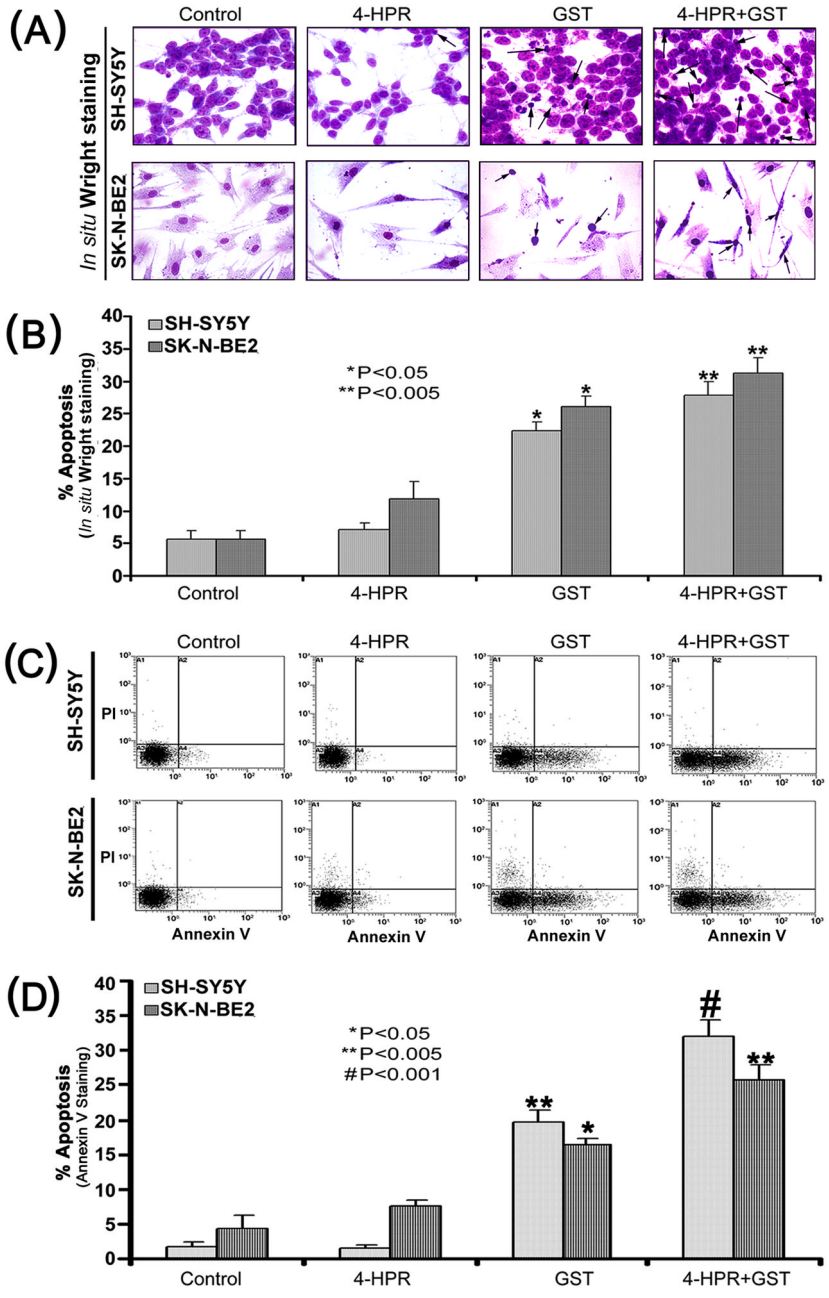

Fig. 4.

Determination of apoptosis in cells after the treatments. Treatments: control, 0.5 μM 4-HPR for 72 h, 25 μM GST for 24 h, and 0.5 μM 4-HPR for 48 h (pretreatment) + 25 μM GST for 24 h. (A) *In situ* Wright staining to examine morphological features of apoptosis. (B) Determination of percentages of apoptosis based on morphological features revealed by Wright Staining. (C) Annexin V staining and flow cytometric analysis of apoptotic populations after the treatments. Flow cytometric data presented here show only one of the three independent experiments in both SH-SY5Y and SK-N-BE2 cell lines. Combination of 4-HPR and GST induced significant population of cells in A4 area, indicating apoptotic death. (D) Determination of percentages of apoptosis based on accumulation of Annexin V positive cells in A4 area.

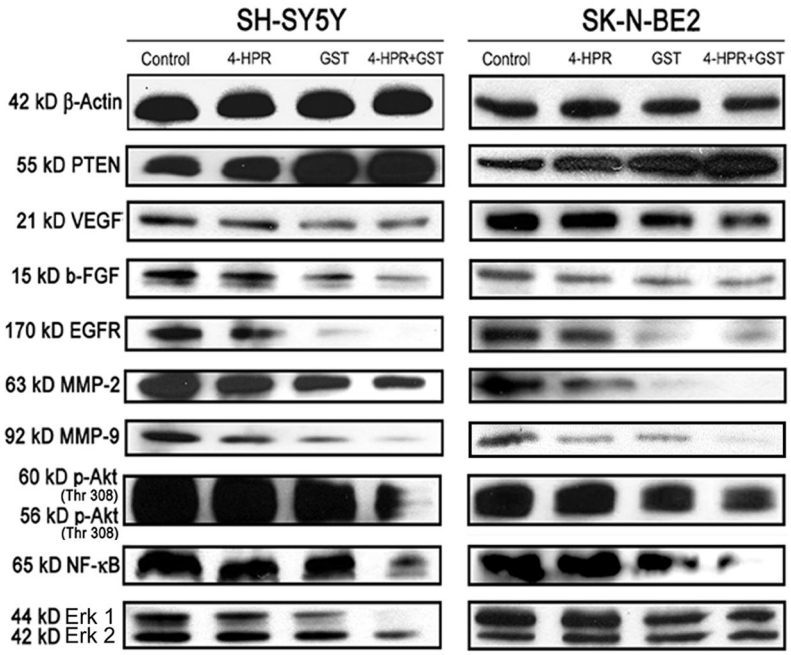

Fig. 5.

Changes in the levels of molecules regulating angiogenic and mitogenic cascades. Treatments: control, 0.5 μM 4-HPR for 72 h, 25 μM GST for 24 h, and 0.5 μM 4-HPR for 48 h (pretreatment) + 25 μM GST for 24 h. Representative Western blots to show changes in levels of PTEN, angiogenic and invasive factors, and also survival factors. Expression of β-actin was used as a loading control. All experiments were conducted in triplicates.

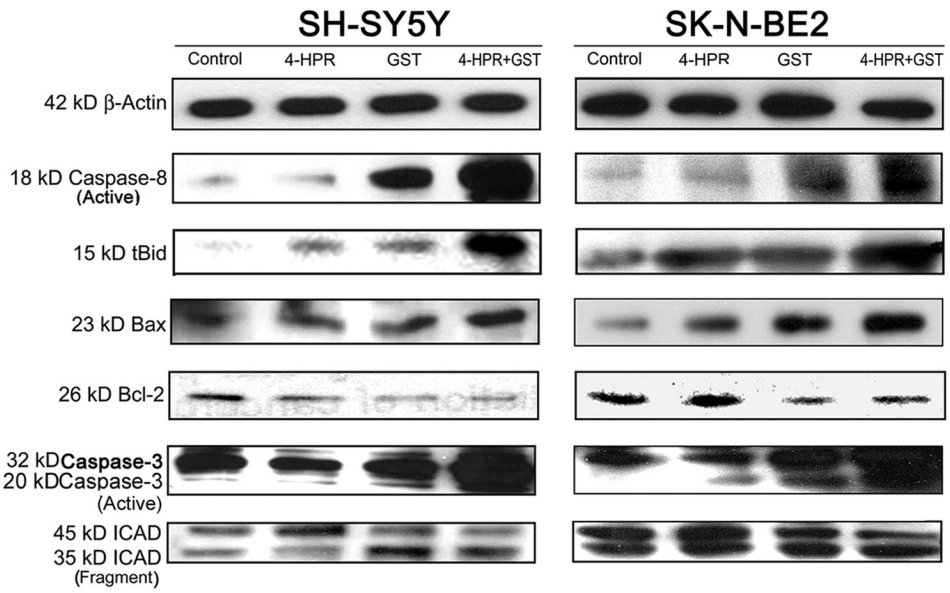

Fig. 6.

Activation of molecular components of the extrinsic and intrinsic pathways of apoptosis. Treatments: control, 0.5 μM 4-HPR for 72 h, 25 μM GST for 24 h, and 0.5 μM 4-HPR for 48 h (pretreatment) + 25 μM GST for 24 h. Representative Western blots to show activation and level of molecules involved in extrinsic and intrinsic pathways of apoptosis. Expression of β-actin was used as a loading control. All experiments were conducted in triplicates.

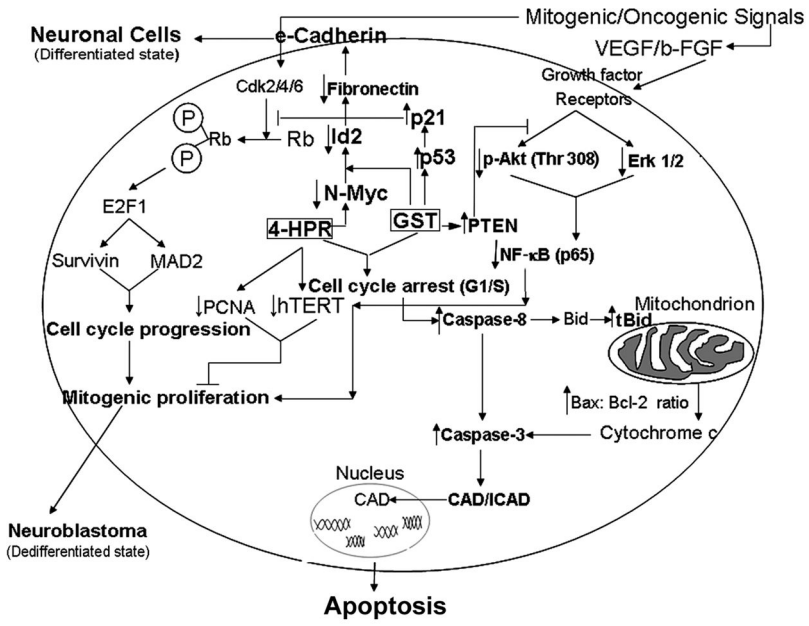

Fig. 7.

Schematic presentation of the molecular components and pathways to show induction of differentiation and apoptosis in neuroblastoma cells. Treatment of cells with 4-HPR induced differentiation with upregulation of the tight junction protein e-cadherin and down regulation of Notch-1, Id2, and fibronectin. Combination of 4-HPR and GST reactivated the expression of tumor suppressors (p53, p21, Rb and PTEN), which inhibited the N-Myc mediated mitogenic/oncogenic signals leading to suppression of cellular proliferation as evidenced by down regulation of hTERT and PCNA. Pretreatment of cells with 4-HPR potentiated GST mediated cell cycle arrest and induction of both extrinsic and intrinsic pathways of apoptosis in neuroblastoma cells.